An Approximate Model for Predicting Roll Force in Rod Rolling

Youngseog Lee*, Hong Joon Kim
Plate, Rod & Welding Group and bSteel Products & Process Group at Technical Research Laboratories, Pohang Iron and Steel Corp. (POSCO), Pohang, Kyungbuk 970-785, Korea
Sang Moo Hwang
Department of Mechanical Engineering, Pohang University of Science and Technology (POSTECH), Pohang, Kyungbuk 970-785, Korea

This paper presents a study of the effect of rolling temperature, roll gap (pass height), initial specimen size and steel grades of specimens on the roll force in round-oval-round pass sequence by applying approximate method and verifications through single stand pilot rod rolling tests. The results show that the predicted roll forces are in good agreement with the experimentally measured ones. The approximate model is independent of the change of roll gap, specimen size and temperature. Thus, the generality of the prediction methodology employed in the approximate model is proven. This study also demonstrates that Shida's constitutive equation employed in the approximate model needs to be corrected somehow to be applicable for the medium and high carbon steels in a lower temperature interval (700~900℃).

Key Words : Approximate Model, Roll Force, Rod (or Bar) Rolling

Nomenclature

A_p : Projected contact area at the interface of workpiece and roll in the roll gap, for plate rolling
A_r : Projected contact area at the interface of workpiece and roll in the roll gap, for rod rolling
C_x, C_y : Coordinate where the roll groove and workpiece are separated each other
F_{plate} : Roll force in plate rolling
F_{rod} : Roll force in rod rolling
G : Roll gap
h_m : Mean height of workpiece in the roll gap
$\bar{h}_m$: Equivalent mean height of the workpiece in the roll gap
$\bar{H}_I$: Equivalent height of incoming workpiece
$\bar{H}_p$: Equivalent height of outgoing workpiece
H_p : Pass height
L : Projected contact length in the roll gap
L_{max} : maximum distance of the projected contact area to the rolling direction
$\bar{L}$: Equivalent projected contact length in the roll gap
N : Roll rpm
R_g : Radius of curvature of round groove
R_I : Radius of curvature of oval groove
$\bar{R}$: Mean roll radius
t_p : Time interval taken for a section A to pass through up to a section C (Fig. 2).
$\bar{W}_I$: Width of equivalent rectangular cross section of the incoming (entry) workpiece
$\bar{W}_p$: Width of equivalent rectangular cross section of the outgoing (exit) workpiece
Y_{avg} : Average flow stress of the workpiece in the roll gap in plane strain condition with strain rate, temperature and carbon content fixed
Y'_{avg} : Average flow stress of the workpiece in the roll gap in uni-axial strain condition

* Corresponding Author,
E-mail : pc554162@posco.co.kr
TEL : +82-54-220-6058; **FAX** : +82-54-220-6911
Plate, Rod & Welding Group at POSCO Technical Research Laboratories, Pohang, Kyungbuk 790-785, Korea. (Manuscript **Received** July 24, 2001; **Revised** December 17, 2001)

with strain rate, temperature and carbon content fixed
α : Relief angle of round groove
ε_i : Principal strain (i=1, 2, 3)
$\bar{\varepsilon}_p$: Mean effective strain
$\dot{\bar{\varepsilon}}$: Mean effective strain rate
μ : Friction coefficient

1. Introduction

For computing the roll forces in rod rolling, a number of numerical studies have been presented on the basis of three-dimensional finite element method (FEM) (Park and Oh, 1990, 1990 ; Kim et al., 1990 ; Shin et al., 1992 ; Komori, 1997 ; Kim et al., 2000). The FEM is very effective in calculating the distribution of plastic deformation of a workpiece and the roll force, but requires at least half an hour to run a program for a single pass since three-dimensional analysis is required in nature. Hence, considering computational time and complicated mechanical/thermal boundary conditions (friction condition at the roll/material interface and heat transfer coefficients dependent on the roll pressure) necessary in the FEM, development of an analytical or approximate method, whch is simple yet with reliable accuracy and non-iterative in computations, has been highly desired.

There were several models for predicting the roll force in rod (or bar) rolling. But those were based on extensive rolling experiments together with empirical coefficients (Wusatowski, 1969 ; Said et al., 1999) and/or regression coefficients (Shinokura and Takai, 1986). Recently, Lee and Kim (2001) proposed the approximate model that computes the roll force in oval-round (or round-oval) pass rolling sequence most commonly employed in rod (or bar) mills. This model excludes any need to conduct a preliminary hot rod rolling experiment to determine a coefficient. The idea behind this model is to approximate a three-dimensional problem into a two-dimensional one by introducing a concept of a weak plane strain condition, which takes into account the deformation characteristics of the work piece during rolling. This exploratory approach (introduction of the concept of the *weak* plane strain condition) was verified for a limited condition (change of rolling temperature). This is the basis of this study.

In this study, investigated is the predicting capability and generality of the approximate model when the i) size of initial specimen ii) roll gap (pass height) and iii) steel grades of specimen are changed. Varying roll gap yields the change of strain at a given pass. Three types of steels, i.e., low (0.1%C), medium (0.45%C), and high (0.72%C) plain carbon steels were employed as specimens. A single stand pilot hot rolling mill was used for rod rolling experiment.

2. Deformation Parameters

The procedure for computing the mean effective strain and strain rate per pass in rod rolling process is outlined, a prerequisite for the calculation of the roll force. The mean effective strain and strain rate are defined as maximum mean effective (equivalent) plastic strain and strain rate at a given pass.

2.1 Calculation of mean effective strain at a pass

To determine the mean effective strain and strain rate per pass, we should first be able to predict the stress free surface profile of the material that does not contact the roll directly at the exit of roll gap. Recently, Lee et al. (2000) developed an analytical model, which is robust and non-iterative in computation, for predicting the surface profile of the exit cross section of a workpiece for the oval-round (or round-oval) pass sequence. Advantage of this model is that only geometric consideration is required in formulation. Hence it greatly simplifies the problem of obtaining the final rolled shape. Figure 1 shows the predicted exit cross sectional profiles and the measured ones for a two-pass rolling sequence. Good agreements were noted between predictions and measurements.

The predicted exit cross section was then transformed into rectangular one, based on the method of maximum width (Lee et al., 2001), as

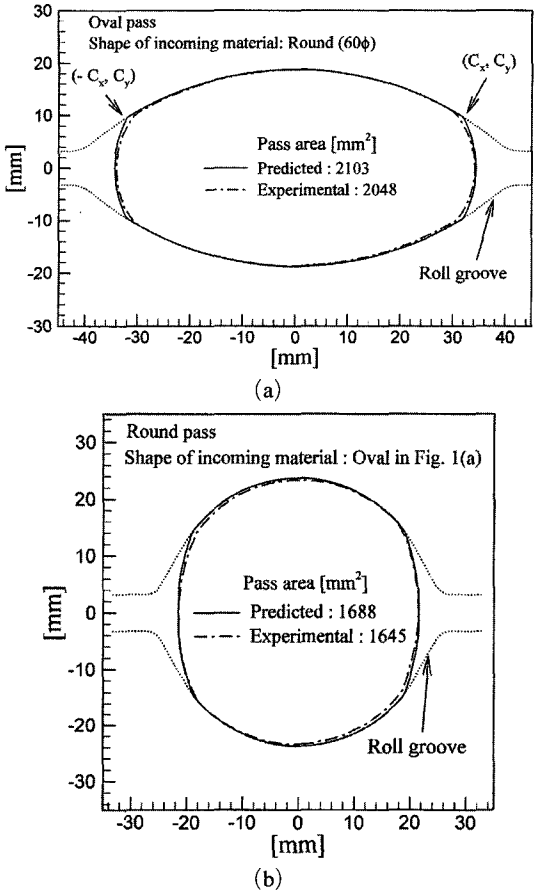

Fig. 1 Predicted and measured surface profile of exit cross sections when a bar with 60mm diameter is rolled into for the two-pass bar rolling sequence. (a) Oval pass and (b) Round pass. C_x and C_y stand for coordinates where the roll groove and workpiece are separated each other at the roll gap position

shown in Fig. 2. Section A, B and C, respectively, corresponds to the positions where a workpiece is about to be rolled, being deformed and leaveing the roll groove, which can be then calculated from the rectilinear shape transformed. Hereafter mean effective strain is referred to as strain. The calculation, however, should include the non-linear change of draught, spread and elongation of material being deformed. The assumption introduced to overcome this problem is the hypothesis of parallelepiped deformation (Wusatowski, 1969).

With the elastic and shear strain components neglected, the incremental plastic deformation

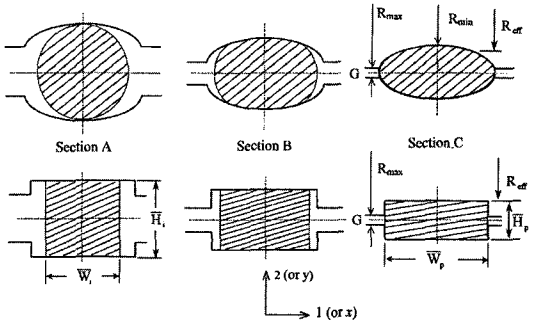

Fig. 2 (a) Schematic description of round-oval pass rolling (front view) (b) Application of equivalent rectangle approximations method to round-oval pass rolling and the mean roll radius, R_{eff}, and equivalent cross sectional heights, $\bar{H}_I$ and $\bar{H}_P$, and equivalent cross sectional widths, $\bar{W}_I$ and $\bar{W}_P$

along each principal axis can be assumed to be proportional, i.e.,

$$d\varepsilon_1 : d\varepsilon_2 : d\varepsilon_3 = \varepsilon_1 : \varepsilon_2 : \varepsilon_3 \tag{1}$$

From the volume constancy condition,

$$\varepsilon_3 = -\varepsilon_1 - \varepsilon_2 \tag{2}$$

Then, the strain at a given pass (i.e., section C in Fig. 2), $\bar{\varepsilon}_p$, is expressed as

$$\bar{\varepsilon}_p = \left[\frac{2}{3}(\varepsilon_1^2+\varepsilon_2^2+\varepsilon_3^2)\right]^{1/2} = \frac{2}{\sqrt{3}}\,\varepsilon_2\left[1+\left(\frac{\varepsilon_1}{\varepsilon_2}\right)^2+\left(\frac{\varepsilon_1}{\varepsilon_2}\right)\right]^{1/2} \ln(\bar{W}_I/\bar{W}_P) \text{ and } \varepsilon_2 = \ln(\bar{H}_I/\bar{H}_P) \tag{3, 4}$$

where $\bar{W}_I$ and $\bar{W}_P$ represent, respectively, the width of equivalent rectangular cross section of the incoming (entry) workpiece and that of the outgoing (exit) workpiece. Similarly, $\bar{H}_I$ and $\bar{H}_P$ stand for the height of equivalent rectangular cross section of the incoming workpiece and that of the outgoing workpiece respectively.

Equation (4) is valid under the assumption that the principal plastic strains in the three principal axes are independent of each other. The positive sign is defined when the workpiece is contracted. Thus, the sign of ε_2 is always positive due to the contraction along y-axis while the sign of ε_1 is negative due to the extension along x-axis. It should be noted that if the ratio $(\varepsilon_1/\varepsilon_2)$ in Eq. (4) is negligibly small, the deformation of the

workpiece in the roll grooves can be approximated by the plane strain condition. As a result, in the course of clarification of complicated three dimensional deformation characteristics during the groove rolling, Eq. (3) can be considered as an extension of the equation for computation of the strain at a pass, being employed in plate rolling theory.

2.2 Calculation of mean effective strain rate at a pass

Similarly in drawing and forging processes, the mean effective strain rate in bar (or rod) rolling changes at various stages of deformation. The mean effective strain rate becomes maximal at the entrance to the roll (or in its vicinity) and begins to decrease along the roll bite, and finally becomes zero at the outlet. For this reason, it is necessary to introduce an "average" strain rate for a given pass. The mean effective strain rate can be defined as the mean effective strain over a time interval which can be calculated from

$$\dot{\bar{\varepsilon}}_p=\bar{\varepsilon}_p/t_p \tag{5}$$

where t_p represents the time interval taken for a section A to pass through up to a section C (Fig. 2). Hereafter mean effective strain rate is referred to as strain rate. The time interval can be expressed as

$$t_p=\frac{60\bar{L}}{2\pi N R_{mean}}[\text{sec}] \tag{6}$$

where R_{mean}, $\bar{L}$ and N are, respectively, the mean roll radius, the equivalent projected contact length of the grooved roll and workpiece, and roll rpm at a given pass. The mean roll radius at a given pass is calculated using the method of maximum width (Lee et al., 2001 ; Lee, 2001). Referring Fig. 2, the equivalent projected contact length is expressed as

$$\bar{L}=\sqrt{\left\{R_{max}-\left(\frac{\bar{H}_p-G}{2}\right)\right\}(\bar{H}_i-\bar{H}_p)} \tag{7}$$

3. Approximate Model of Roll Force

Recently, Lee and Kim (2001) proposed an approximate model which computes the roll force associated with rod (or bar) rolling. Introduced was the concept of the weak plane strain condition so that we can reduce the three dimensional problem in rod rolling into a two dimensional problem. The description of the new terminology can be summarized as follows:

Plane strain condition:
$\varepsilon_1=0$, for plate (or strip) rolling
Weak plane strain condition:
$\varepsilon_1\neq0$, for rod (or bar) rolling.

ε_1 represents the principal plastic strain in the roll axis direction. It means that the deformation resistance of workpiece in the roll axis direction becomes weak when the ratio of width to height of the workpiece cross-section is not large enough, i.e., $\varepsilon_1\neq0$. The deformation behavior under "*weak* plane strain condition" is, in fact, three dimensional one. Nonetheless, we assume that *weak* plane strain condition can be an extension of the plane strain condition so that we can modify the equation for calculating the roll force being used in plate rolling theory. Deductive logic has been used to prove this exploratory approach.

The equation for calculating the roll force under plane strain deformation condition which is used in plate rolling is expressed as (Roberts, 1983 ; Song et al., 1996);

$$\begin{aligned}F_{plate}&=A_p.\ Y_{avg.}\ \exp[(\mu L/h_m)-1]\\&\approx A_p.\ Y_{avg.}\ \exp[\mu L/2h_m]\end{aligned} \tag{8}$$

where μ : Friction coefficient,
Y_{avg} : Average flow stress of the workpiece in the roll gap in plane strain condition with strain rate, temperature and carbon content fixed,
A_p : Projected contact area at the interface of workpiece and roll in the roll gap,
L : Projected contact length in the roll gap,
h_m : Mean height of workpiece in the roll gap.

At this point, we know that the roll force in rod rolling ($\varepsilon_1\neq0$) is always smaller than that in plate rolling ($\varepsilon_1=0$) because the non-zero state

of principal plastic strain to the roll axis direction, i.e., $\varepsilon_1 \neq 0$, makes the deformation of the workpiece much easier than does the zero state of principal plastic strain to the roll axis direction, i. e., $\varepsilon_1 = 0$. Thus, with the concept of the *weak* plane strain condition, the roll force in oval -round (or round-oval) rolling sequence can be formulated by modifying Eq. (8)

$$F_{rod} = (1-\varepsilon_1) \cdot A_r \cdot \frac{2}{\sqrt{3}} \cdot Y'_{avg} \cdot \exp[\mu \bar{L}/2\bar{h}_m] \quad (9)$$

where Y'_{avg}: Average flow stress of the workpiece in the roll gap in uni-axial strain condition with strain rate, temperature and carbon content fixed,

$A_r = 2 \cdot \int_0^{C_x} L_{max} \cdot \left(1 - \frac{x}{C_x}\right)^{1/3} dx$:
Projected contact area at the interface of workpiece and roll groove at the roll gap,

$\bar{L} = \sqrt{\{R_{max} - (\bar{H}_p - G)/2\}(\bar{H}_1 - \bar{H}_p)}$:
Equivalent projected contact length in the roll gap,

$\bar{h} = [(\bar{H}_1 + \bar{H}_p)/2]$:
Equivalent mean height of the workpiece in the roll gap.

The term, $(1-\varepsilon_1)$, $\bar{L}$ and $\bar{h}_m$ in Eq. (9), highlights the difference between the roll force model for rod rolling and one for plate rolling. Introduction of this term stems from a need to take a simplified treatment to the deformation characteristics of the workpiece at the inside of the roll groove, using a temperature and strain rate independent deformation parameter. That is, the roll force can be modeled to be reducing in proportional to ε_1, i.e., the natural logarithmic of the ratio of the increment of spread (in the roll axis direction) of the workpiece at the entry and exit of roll gap if the projected contact length and mean height of the workpiece in the roll gap have an equivalent form, as shown in Eq. (9).

Figure 3 shows an example of the projected contact area at the interface of workpiece and roll groove at the roll gap. These were acquired by the emergency stop of the pilot rod rolling mill. The white line distinguishes the portion in contact.

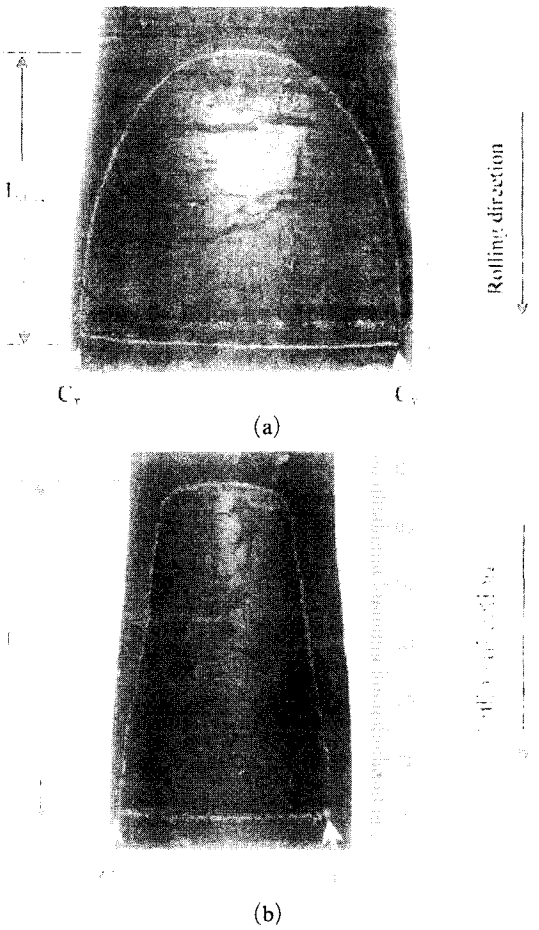

Fig. 3 Shape of projected contact area of workpiece deformed inside of roll groove and its geometric designation when a specimen with 60mm diameter is rolled. (a) Oval pass and (b) Round pass. C_x, and C_y are coordinates where the roll groove and workpiece are separated each other at the roll gap position. The pass sequence is described in Fig. 4

L_{max} represents the maximum distance of the projected contact area to the rolling direction. It is worth noting that even though the shapes of projected contact area are different for each pass, a single integral equation with a polynomial function is enough to compute the projected contact area for both passes.

The flow stress of workpiece was characterized by Shida's constitutive equation (Shida, 1969), giving the flow stress as a function of the carbon content, the strain, the strain rate and tempera-

ture. This equation was chosen primarily due to its simplicity in applications. In addition, it also takes account of the flow stress behavior of the steels in austenite, ferritic and in the two-phase regions. This fact is a forte of Shida's constitutive equation in comparison with the other constitutive equations (Lenard et al., 1999). The range of validity of the formula is quite broad. This formula is applicable for plain carbon steel in the range of carbon content: 0.07～1.2%, temperature: 700～1200[℃], strain rate: 0.1～100[1/s] and strain: up to 0.7.

In metalworking process, the determination of a coefficient of friction is quite difficult since it is a function of the rolling load, temperature, speed, properties of the workpiece and lubricant condition at the groove/workpiece interface. Therefore the coefficient of friction was considered to be in the wide range (0.2～0.7) in hot rolling condition (Kalpakjian, 1992). In this study, the coefficient of friction between the work rolls and the workpiece was assumed to be 0.4. It is worth mentioning that a choice of the coefficient of friction may take very minor effect on the prediction of the roll force.

4. Experiment

4.1 Rolling equipment and specimen preparation

A single stand two-high laboratory mill was employed, driven by 75kW constant torque, DC motor. DCI (Ductile Casting Iron) rolls were used, with 310mm maximum diameter and 320mm face width. The rolling speed was set at 0.5m/s (34rpm). A box type furnace with the maximum working temperature of 1400℃ was employed to heat up the specimens to the desired rolling temperature. Low, medium and high carbon steels with a chemical composition of Fe-0.1C-0.45Mn-0.25Si (wt.%), Fe-0.45C-0.75Mn-0.25Si (wt.%) and Fe-0.72C-0. 45Mn-0.25Si (wt.%) were used. The material was obtained in the form of square as-cast billet with a side length of 160mm. The specimens to be rolled were cut and machined into a round bar with 60mm diameter and 300mm length.

4.2 Experimental procedure

For rolling experiments, specimens were soaked at 1130℃ for 1 hour to ensure a homogenous temperature distribution. They were taken out of the furnace and when the center temperature of specimens reached 1100℃, 950℃ and 800℃, respectively, the tests were conducted. In order to measure the rolling temperature of workpiece, a thermocouple (type K) with 1. 6mm diameter was embedded in 50mm deep holes drilled in the tail ends of the specimen. The roll has a round groove and an oval groove as shown in Fig. 4.

A specimen was first rolled into the oval pass [Fig. 4(a)] at the desired temperature and cooled in air to room temperature. For the round pass rolling, the workpiece was re-heated up to the desired temperature in the furnace. The oval shape workpiece was then rolled into the round pass [Fig. 4(b)] after it was rotated 90 degree about the length direction. Entrance guides were installed in front of the roll groove to minimize sideway bending of specimen. The roll forces were measured by using two force transducers during rolling, located over the bearing blocks of the top work roll. To assure the credibility of

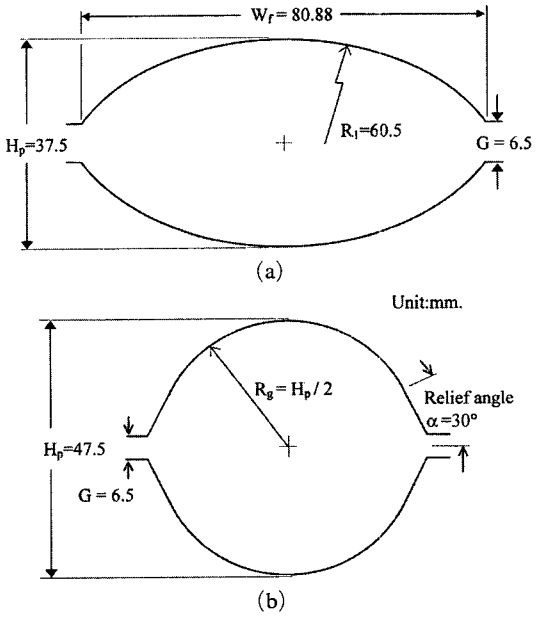

Fig. 4 Roll groove shape and design parameters used for the two-pass bar rolling sequence. (a) Oval pass and (b) Round pass

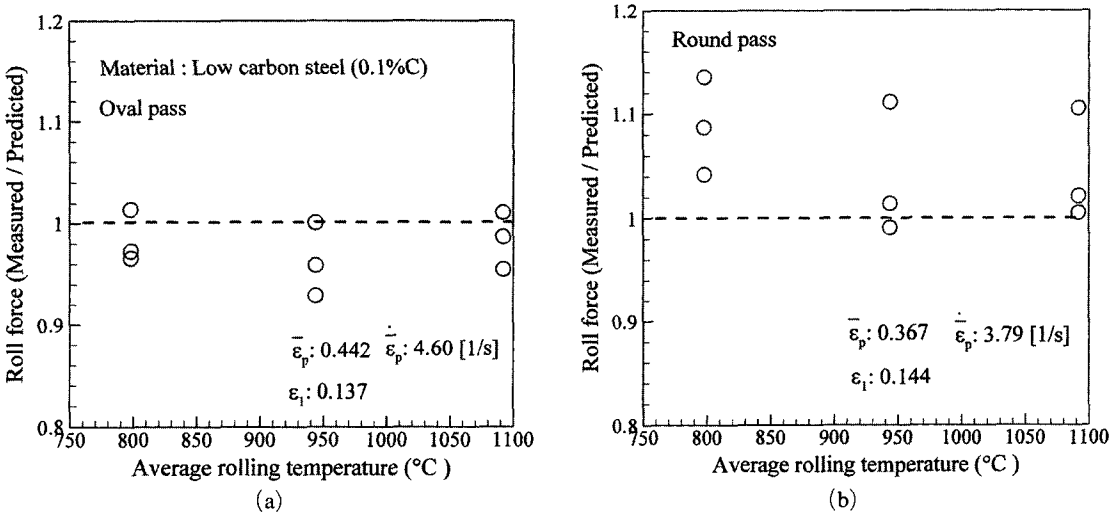

Fig. 5 Comparison of the predicted and measured roll forces for low carbon steel (0.1%C) for the two-pass bar rolling sequence when the temperature of specimen is changed. (a) Oval pass and (b) Round pass.

experimental data, the experiment was repeated three times under the same rolling condition.

5. Results and Discussion

5.1 Effect of rolling temperature on the approximate model

The temperature of the specimen is uniform whilst in the closed furnace. As soon as it is removed from the furnace, the surface begins to cool at a faster rate than at the center. The properties of the specimens depend on the cooling rate in addition to the heated temperature. Since the former varies across the cross-section, a homogeneous property is not obtained across the cross-section. Therefore, average temperature of the specimen is used when calculating the flow stress of the specimen.

Figure 5 illustrates the normalized roll forces at the oval pass and round pass, respectively, when the rolling temperature of workpiece varies. The approximate model combined with Shida's constitutive equation (Song et al., 1996) is shown to be independent of the rolling temperature for low carbon steel. For the oval pass rolling, the roll forces predicted from the proposed approximate model overvalue slightly those experimentally measured. For the round pass rolling, however, opposite results are observed. The differences between the measured and the predicted roll forces at each temperature are in the range of 1.5~ −7.5% for the oval pass rolling and 13.5~ −1% for the round pass rolling, respectively. In the round pass, some fluctuations in the measured roll force are observed. This might be due to unstable rolling when the specimen with an oval shape is rolled at the round pass, compared with relatively stable rolling when the one with a round shape is rolled at the oval pass.

5.2 Effect of change of roll gap on the approximate model

Figure 6 shows the normalized roll forces when the roll gap (pass height) at the oval pass and the round pass, respectively, varies. The rolling temperature is fixed at 950℃. When the roll gap (pass height) is changed, the mean effective strain is changed and subsequently the strain component to the roll axis direction, ε_l, also varies (See Fig. 2). The differences between the measured and predicted roll forces start to increase as the roll gap varies. Deviation is large at the round pass. In case of the round pass, the approximate model is influenced somewhat by the variation of strain (i.e., pass height) at a pass. In the present study, the roll gap at each pass has been changed up to ±61.5%. In general, the process designer or operator in mill yard does not change the roll gap

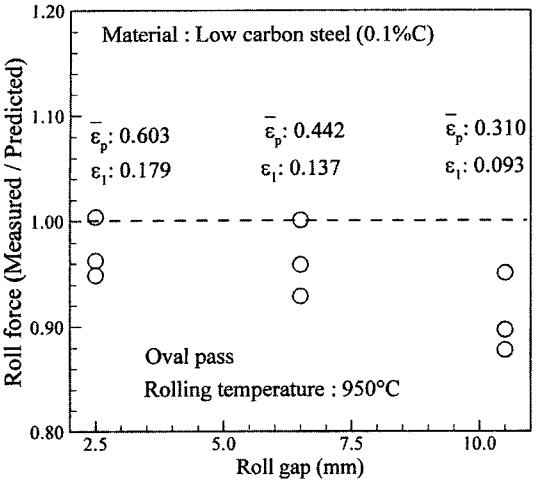

(a)

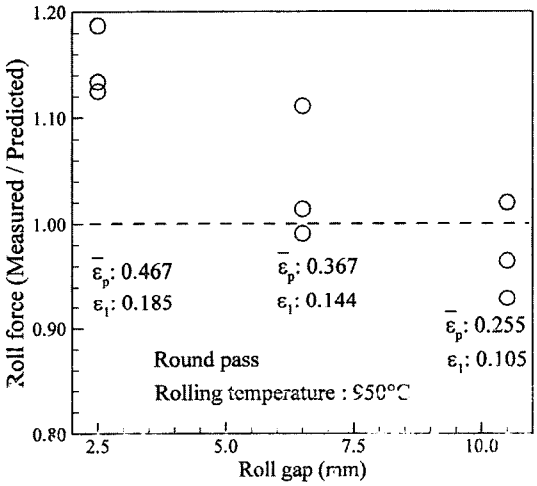

(b)

Fig. 6 Comparison of the predicted and measured roll forces for low carbon steel (0.1%C) when the roll gap (pass height) is changed. ε_1 represents the principal plastic strain to roll axis direction. (a) Oval pass and (b) Round pass

in round pass as drastically as demonstrated in this study.

5.3 Effect of change of initial specimen size on the approximate model

Figure 7 shows the normalized roll forces when the size of initial specimen is changed (from 60mm to 66mm in diameter). The rolling temperature is fixed at 950℃. Almost the same phenomenon, which was shown in Fig. 6, is observed

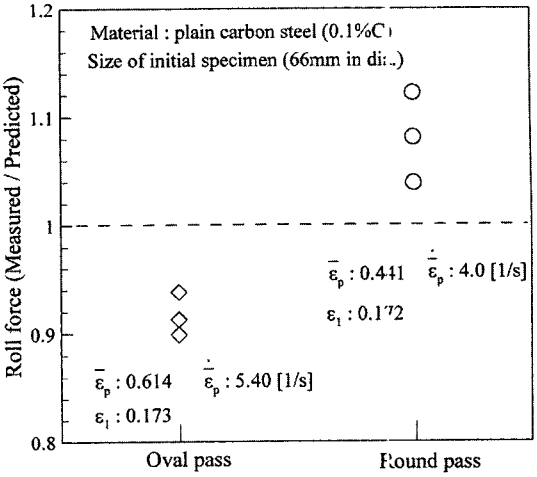

Fig. 7 Comparison of the predicted and measured roll forces for low carbon steel (0.1%C) when the size of initial specimen is changed (from 60mm to 66mm in diameter). The rolling temperature is fixed at 950℃. (a) Oval pass and (b) Round pass

since the variation of initial specimen size leads the change of the strain at a pass. In oval pass, the measured roll forces are slightly lower that the predicted one. Meanwhile, opposite results are observed in round pass. In overall, the roll forces predicted are in agreement with the one measured when even the incoming specimen size is changed.

5.4 Effect of carbon content of steel on the approximate model

To examine the predictive capabilities of the approximate model to the carbon contents of steels, medium carbon (0.45%C) and high carbon (0.72%C) steels were also rolled. Note that the previously published works (Said et al., 1999; Shinokura and Takai, 1986) for predicting and measuring the roll forces was limited to low carbon (0.18~0.2%C) steels.

The measured roll forces and predicted ones are compared in Figs. 8 and 9. It demonstrates that the roll forces predicted by the approximate model overvalue slightly those experimentally measured. In comparison with the case of low carbon steel, differences at the temperature of 1100℃ and 950℃ are acceptable. But as the tem-

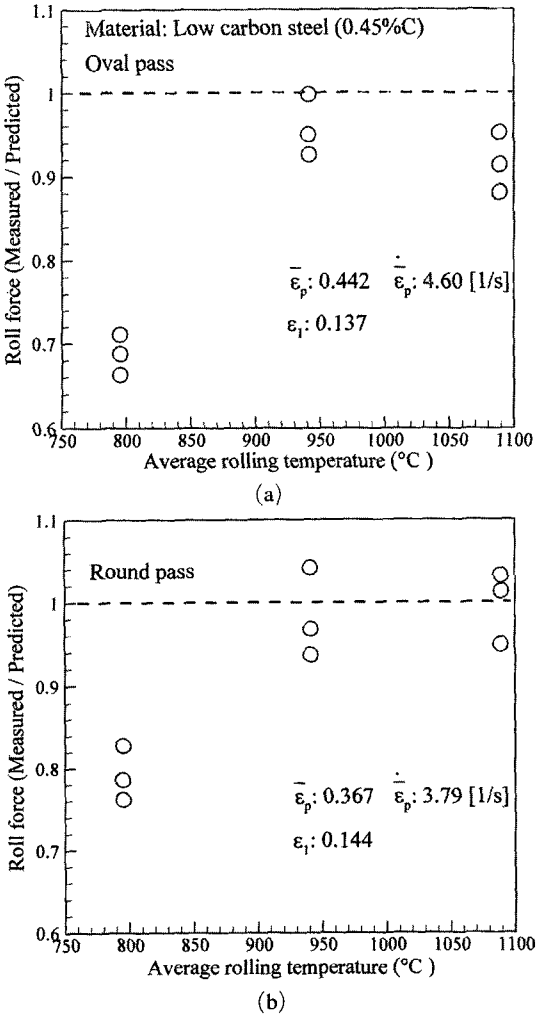

Fig. 8 Comparison of the predicted and measured roll forces of medium carbon steel (0.45%C) for the two-pass bar rolling sequence (a) Oval pass and (b) Round pass

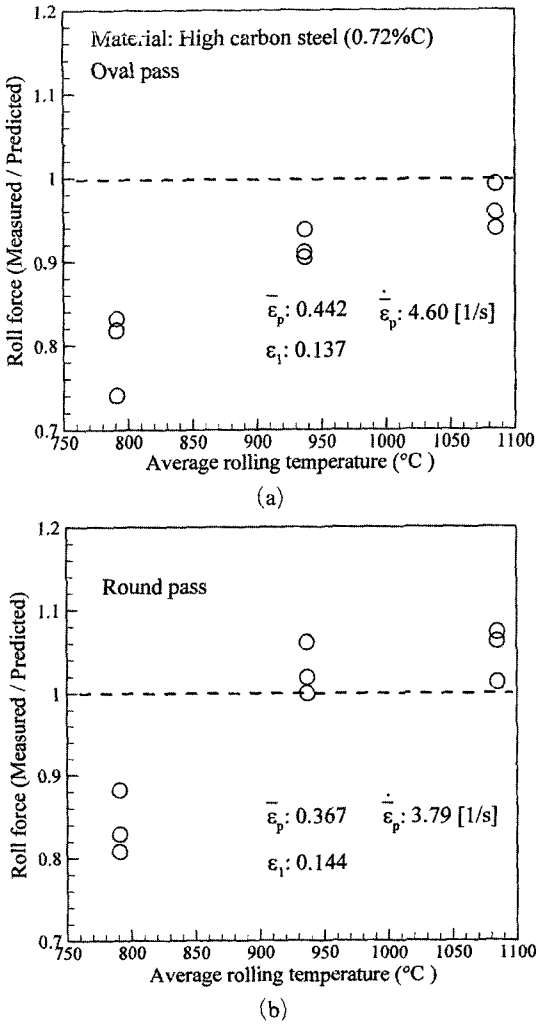

Fig. 9 Comparison of the predicted and measured roll forces of high carbon steel (0.72%C) for the two-pass bar rolling sequence (a) Oval pass and (b) Round pass

perature decreases to about 800℃, the predicted roll forces for both passes increase significantly. Note that the exit cross sectional shape and area of deformed workpiece for the medium and high carbon steel showed almost no difference in comparison with those for the low carbon steel (Lee and Kim, 2001).

To study the influence of the carbon contents of steels on the roll force prediction at lower temperatures, the sensitivity of Shida's constitutive equation to the carbon content and temperature variation has been investigated. The results are given in Fig. 10, which shows the steel's deformation resistance (flow stress) as a function of the temperatures for the various carbon contents, with the deformation parameters (strain and strain rate) used in the oval pass fixed. The strength of the austenite appears to be independent of the carbon content. As the temperature decreases, the flow stress of the steel increases in an exponential form. When the temperature indicating the appearance of the first ferrite regions reached, the strength falls sharply with further temperature drop. After the end of the phase

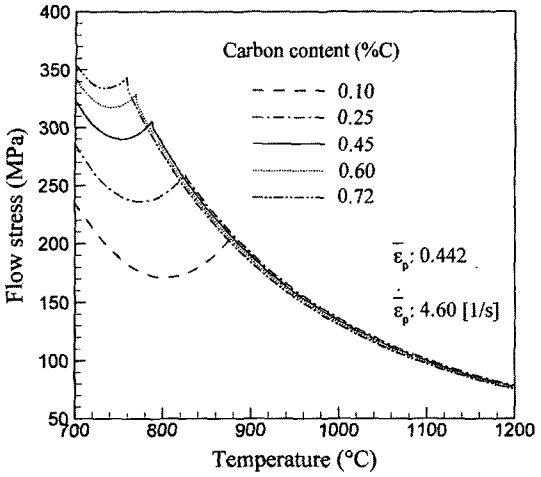

Fig. 10 Temperature dependence of the flow stress (deformation resistance) of steels as a function of carbon content at a fixed strain and strain rate, used in the oval pass

transformation, the strength increases again.

Since, as observed in Figs. 8 and 9, the measured roll forces is about 20~30% lower than the predicted ones, it may be deduced that the gradient of flow stress increment ($\partial\bar{\sigma}/\partial\bar{\varepsilon}_p$) in Shida's constitutive equation, accompanying with the temperature decrement, might be lower than that Shida had proposed. In other words, Shida's constitutive equation might overvalue the flow stress of the medium and high carbon steel in a lower temperature interval (say, 700~900℃). This may be attributed to the cooling rate of specimen used in this rolling experiment and Shida's hot compression test, and degree of inhomogeneous temperature distribution across specimen just before the rolling experiment and compression test. Therefore, further research might be needed to examine Shida's constitutive equation for the medium and high carbon steel that are in line with the hot compression test.

6. Concluding Remarks

The concept of a *weak* plane strain condition, which reduces the three-dimensional deformation problem into a two-dimensional one, has been introduced to formulate the approximate model that predicts the roll force in rod (or bar) rolling. The generality and predictive capabilities of the model combined with Shida's constitutive equation have been examined by hot rod rolling experiment, with the i) roll gap (pass height), ii) size of initial specimen and iii) steel grades of specimens changed. The conclusions are summarized as follows:

(1) The roll forces predicted from the approximate model are in good agreement with those experimentally measured even when those roll parameters vary. Thus, the prediction methodology by introduction of the concept of the *weak* plane strain condition is proven valid.

(2) The approximate model is also shown to be independent on the steel grades. But, for medium and high carbon steels at the temperature of around 800℃, the predicted roll forces are greater (20~30%) than those experimentally measured. Further study might be needed to examine Shida's constitutive equation for the medium and high carbon steels by making the specimen smaller and varying the cooling rate of specimen.

References

Kalpakjian, S., 1992, "*Manufacturing Processes for Engineering Materials-2nd ed.*," Addison Wesley Publishing Company, pp. 171~175.

Kim, H. J., Kim, T. H. and Hwang, S. M., 2000, "A New Free Surface Scheme for Analysis of Plastic Deformation in Shape Rolling," *J. Mater. Proc. Tech.*, Vol. 24, pp. 81~93

Kim, N., Lee, S. M., Shin, W. and Shivpuri, R., 1990, "Simulation of Square-to-Oval Single Pass Rolling Using a Computationally Effective Finite and Slab Element Method," *J. Eng. Ind.*, Vol. 114, pp. 329~335.

Komori, K., 1997, "Simulation of Deformation and Temperature in Multi-Pass Caliber Rolling," *J. Mater. Proc. Tech.*, Vol. 71, pp. 329~336.

Lee, Y., 2001, "An Analytic Study of Mean Roll Radius in Rod Rolling," *ISIJ Int.*, Vol. 41, pp. 1416~1418.

Lee, Y. and Kim, B. M., 2001, "Prediction of the Surface Profile of Exit Cross Section in Round-Oval-Round Pass Rolling Sequence," Accepted for publication in KSME International.

Lee, Y., Choi, S. and Kim, Y. H., 2000, "Mathematical Model and Experimental Validation of Surface Profile of a Workpiece in Round-Oval-Round Pass Sequence," *J. Mater. Proc. Tech.*, Vol. 81, pp. 87~96.

Lee, Y., Kim, H. J. and Hwang, S. M., 2001, "Analytic Model for the Prediction of Mean Effective Strain in Rod Rolling Process," *J. Mater. Proc. Tech.*, Vol. 114, pp. 129~138.

Lee, Y. and Kim, Y. H., 2001, "Approximate Analysis of Roll Force in Round-Oval-Round Pass Rolling Sequence", *J. Mater. Proc. Tech.*, Vol. 113, pp. 124~130.

Lenard, J. G., Pietrzyk, M. and Cser, L., 1999, "*Mathematical and Physical Simulation of the Properties of Hot Rolled Products*," Elsevier Science Ltd., Netherlands, pp. 73~75.

Park, J. J. and Oh, S. I., 1990, "Application of Three Dimensional Finite Element Analysis to Shape Rolling Process," *J. Eng. Ind.*, Vol. 112, pp. 36~46.

Roberts, W. L., 1983, *Hot Rolling of Steel*, Marcel Dekker Inc, New York, pp. 687~689.

Said, A., Lenard, J. G., Ragab, A. R. and Elkhier, M. A., 1999, "The Temperature, Roll Force and Roll Torque During Hot Bar Rolling," *J. Mater. Proc. Tech.*, Vol. 88, pp. 147~153.

Shida, S., 1969, "Empirical Formula of Flow Stress of Carbon Steels-Resistance to Deformation of Carbon Steels at Elevated Temperature," 2nd Report (in Japanese), *J. JSTP*, Vol. 10, pp. 610~617.

Shinokura, T. and Takai, K., 1986, "Mathematical Models of Roll Force and Torque in Steel Bar Rolling," (in Japanese), *ISIJ Int.*, Vol. 72, pp. 58~64.

Shin, W., Lee, S. M., Shivpuri, R. and Altan, T., 1992, "Finite-Slab Element investigation of Square-to-Round Multi-Pass Shape Rolling," *J. Mater. Proc. Tech.*, Vol. 33, pp. 141~154.

Song, G. H., Kim, S. I. and Park, H. D., 1996, "A Study of Improvement of Prediction Accuracy for Rolling Force in Continuous Rolling Mill," *Trans. KSME* (in Korean), Vol. 20, pp. 2257~2265.

Wusatowski, Z., 1969, *Fundamentals of Rolling*, Pergamon Press, London, pp. 107~109.